https://doi.org/10.1093/plphys/kiac040 PLANT PHYSIOLOGY 2022: 189: 188–203

Plant Physiology®

Research Article

Rapid stomatal closure contributes to higher water use efficiency in major C_4 compared to C_3 Poaceae crops

Kengo Ozeki,[1] Yoshiyuki Miyazawa[2] and Daisuke Sugiura [1,*,†]

1 Graduate School of Bioagricultural Sciences, Nagoya University, Chikusa, Nagoya 464-8601, Japan
2 Campus Planning Office, Kyushu University, Nishi, Fukuoka 819-0395, Japan

*Author for correspondence: daisuke.sugiura@gmail.com
†Senior author.

D.S. and K.O. designed the experiments, D.S. and K.O collected the data, D.S. and Y.M analyzed the data, and D.S. wrote the manuscript.
The author responsible for distribution of materials integral to the findings presented in this article in accordance with the policy described in the Instructions for Authors (https://academic.oup.com/plphys/pages/general-instructions) is: Daisuke Sugiura (daisuke.sugiura@gmail.com).

Abstract

Understanding water use characteristics of C_3 and C_4 crops is important for food security under climate change. Here, we aimed to clarify how stomatal dynamics and water use efficiency (WUE) differ in fluctuating environments in major C_3 and C_4 crops. Under high and low nitrogen conditions, we evaluated stomatal morphology and kinetics of stomatal conductance (g_s) at leaf and whole-plant levels in controlled fluctuating light environments in four C_3 and five C_4 Poaceae species. We developed a dynamic photosynthesis model, which incorporates C_3 and C_4 photosynthesis models that consider stomatal dynamics, to evaluate the contribution of rapid stomatal opening and closing to photosynthesis and WUE. C_4 crops showed more rapid stomatal opening and closure than C_3 crops, which could be explained by smaller stomatal size and higher stomatal density in plants grown at high nitrogen conditions. Our model analysis indicated that accelerating the speed of stomatal closure in C_3 crops to the level of C_4 crops could enhance WUE up to 16% by reducing unnecessary water loss during low light periods, whereas accelerating stomatal opening only minimally enhanced photosynthesis. The present results suggest that accelerating the speed of stomatal closure in major C_3 crops to the level of major C_4 crops is a potential breeding target for the realization of water-saving agriculture.

Introduction

Due to climate change and population growth, it will become increasingly difficult to secure agricultural water for crop production, which accounts for 70% of the world freshwater use (Hirabayashi et al., 2013; Carrão et al., 2016). Therefore, understanding the water use characteristics of major Poaceae crops, which provide >60% of the world food production, is essential for forecasting future water demand and for the improvement of crop water use efficiency (WUE) (Condon, 2020).

Plant water use and photosynthesis are strongly determined by transpiration and CO_2 uptake through stomata. Since about 99% of water absorbed by roots are lost by transpiration, plants strictly regulate stomatal movement in response to dynamic environmental conditions and according to physiological status (Lawson and Vialet-Chabrand, 2019; Lawson and Matthews, 2020). Leaf-level stomatal responses to various environmental cues and underlying physiological and molecular mechanisms have been well investigated (Shimazaki et al., 2007), while plant- to canopy-

Received August 13, 2021. Accepted December 08, 2021. Advance access publication February 3, 2022

level water use in fluctuating environments are not. This suggests that there is still potential for improving irrigation management and developing water-saving cultivars of major cereal crops as staple food sources.

Generally, C_4 plants exhibit higher photosynthetic rate (A) and lower stomatal conductance (g_s) relative to their high A compared with C_3 herbaceous plants, which was achieved by the CO_2 concentrating mechanism (Dai et al., 1993). Consequently, C_4 plants show higher leaf-level WUE calculated as the ratio of maximum A (A_{max}) to maximum g_s or maximum transpiration rate (E) when compared among C_3 and C_4 grasses (Osborne and Sack, 2012; Way et al., 2014). C_4 plants are classified into three subtypes based on the dominant C_4 acid decarboxylation enzymes (Gutierrez et al., 1974), and all the three subtypes are shown to have high leaf-level WUE (Cano et al., 2019). It is also reported that C_4 and C_4-like species showed higher leaf-level WUE than C_3 species and C_3–C_4 intermediates of *Flaveria* species (Vogan and Sage, 2011). Furthermore, whole-plant WUE calculated as the ratio of dry mass to cumulative water use are about two-times higher in C_4 plants than in C_3 plants (Shantz and Piemeisel, 1927; Ghannoum et al., 2002; Igarashi et al., 2021). In these studies, leaf-level WUE as the ratio of A_{max} to maximum g_s (or E) at the steady state or whole-plant WUE at the harvest were evaluated, which have deepened our understanding of the differences in leaf-level and whole-plant WUE and drought tolerance among C_3 and C_4 plants (Leakey et al., 2019). However, A and g_s rarely reach steady-state maximum values since light intensity, air temperature, and vapor pressure deficit (VPD) fluctuate greatly even under open field conditions due to solar angle, wind, sun and shade flecks, and self- and mutual shading (Pearcy, 1990; Miyashita et al., 2012; Lawson and Vialet-Chabrand, 2019). Furthermore, it is also important to evaluate whole-plant water use, which reflect plant form and light-intercepting characteristics to reveal what stomatal dynamics contribute to the higher leaf-level and whole-plant WUE under field conditions from an agronomic point of view (Monsi and Saeki, 2005). Recently, several studies have investigated dynamics of stomatal responses in fluctuating light in mutant and over expression lines of *Arabidopsis thaliana* and rice (*Oryza sativa*; Yamori et al., 2020; Kimura et al., 2020) and across plant functional types (Vico et al., 2011) or cultivars (Qu et al., 2016). McAusland et al. (2016) investigated stomatal kinetics and morphology in 15 plant species including 3 upland C_3 crops (wheat [*Triticum aestivum*], barley [*Hordeum vulgare*], and oat [*Avena sativa*]) and 2 C_4 crops (sorghum (*Sorghum bicolor*) and maize (*Zea mays*)), showing that Poaceae species exhibit faster stomatal responses than dicotyledonous crops. Several studies also reported that maize, sorghum, and other C_4 grasses show rapid stomatal responses under light fluctuations (Bellasio et al., 2017; Wang et al., 2021). These findings suggest that higher WUE of C_4 crops may be attributed to rapid stomatal responses, which could be an important breeding target for improving the WUE of C_3 crops. However, these findings are still limited to the leaf-level responses, and no study has compared leaf-level and whole-plant stomatal dynamics among major C_3 and C_4 crops. Although guard cell size is regarded as one of the key determinants of stomatal kinetics (Elliott-Kingston et al., 2016), little is known about the relationship between them among major C_3 and C_4 crops (Taylor et al., 2012). Nitrogen (N) is another key determinant of g_s since plants grown under high nitrogen (HN) availability with higher leaf nitrogen content showed higher A and g_s in both C_3 and C_4 species (Evans, 1989; Ghannoum et al., 2011). However, studies on how leaf nitrogen content influences stomatal kinetics at leaf and whole-plant levels in C_3 and C_4 crops are lacking. From a viewpoint of fertilization and water management in agriculture, it is important to clarify the effect of nitrogen fertilization level on stomatal kinetics in major C_3 and C_4 Poaceae crops.

Heat-based sap flow techniques such as the thermal dissipation method (Granier, 1987) and the heat ratio method (Clearwater et al., 2009) have been developed to evaluate plant water use continuously under variable field conditions. However, these methods require calibration of heat pulse velocity by gravimetrically measured water consumption and have difficulties in data collection at fine time resolutions, making these methods difficult to apply for the accurate estimation of stomatal conductance in response to short-term fluctuations of light intensity, wind, air temperature, and VPD. In addition to measuring leaf-level gas exchange by the portable photosynthesis system, we aimed to address the above issues by developing a system which enables the continuous measurement of whole-plant water consumption using electronic balances with Bluetooth communication function in controlled fluctuating LED conditions. Although whole-plant water use is evaluated gravimetrically by weighing pot weights in many studies, few studies has quantified whole-plant stomatal conductance by continuous measurements of water consumption at a fine time scale to characterize stomatal kinetics (Douthe et al., 2018; Eyland et al., 2021). Furthermore, while most studies have focused on the photosynthetic induction process via stomatal opening in response to the increased light intensity (Lawson and Vialet-Chabrand, 2019), the present study particularly focuses on the stomatal closure in response to decreased light intensity and its contribution to an increase in WUE by reducing unnecessary water loss during low light period. Here, we tested a hypothesis that C_4 crop species with higher drought tolerance would show rapid stomatal closure in response to low light period to minimize unnecessary water loss, which could contribute to higher WUE of C_4 crops. Since photosynthesis is limited by electron transport rather than stomatal conductance during low light period (Farquhar et al., 1980), rapid stomatal closure does not decrease CO_2 assimilation but should substantially reduce water consumption. To test the hypothesis, a model that incorporates the C_3 and C_4 photosynthesis models with stomatal dynamics was developed. Using the model, we simulated how much photosynthesis and water consumption

could be affected by accelerating/decelerating stomatal opening/closure in fluctuating light environments in the C_3 and C_4 species. In the present study, we selected four C_3 and five C_4 major Poaceae crops, and they were grown under high and low nitrogen (LN) availability to evaluate leaf-level and whole-plant stomatal dynamics and stomatal morphology.

Results

Leaf-level physiological and morphological traits

Dynamics of leaf-level photosynthetic characteristics, g_s and WUE, to the fluctuating light were clearly different between the C_3 and C_4 Poaceae species (Figures 1 and 2). The dynamics of A was similar between the C_3 and C_4 species as it reached A_{max} during the high light period and dropped at the beginning of the low light period (Figure 1, A–D, I–M). On the other hand, the shape of g_s dynamics differed markedly between the C_3 and C_4 species. The C_3 species showed slow change in g_s in response to the start of both low and high light period (Figure 1, E–H), whereas C_4 species showed rapid change in g_s (Figure 1, N–Q) except for *Z. nicaraguensis* (Figure 1R), leading to the quite different dynamics of leaf-level WUE (Figure 2). WUE was higher in the C_4 species than the C_3 species during the high light period. After WUE dropped in the beginning of the low light period in both C_3 and C_4 species, WUE gradually increased in most of the C_3 species (Figure 2, A–D), whereas it rapidly increased to the values under the high light period in most of the C_4 species (Figure 2, E–I). As a result, the C_4 species showed significantly higher WUE_{HL} and WUE_{LL} than the C_3 species (Table 1).

From the quantitative analysis of leaf-level stomatal dynamics, k_{open} and k_{close} were markedly different among species (Figure 3), and they were significantly different between the C_3 and C_4 species at each soil nitrogen condition (Supplemental Table S1). k_{open} and k_{close} were smallest in

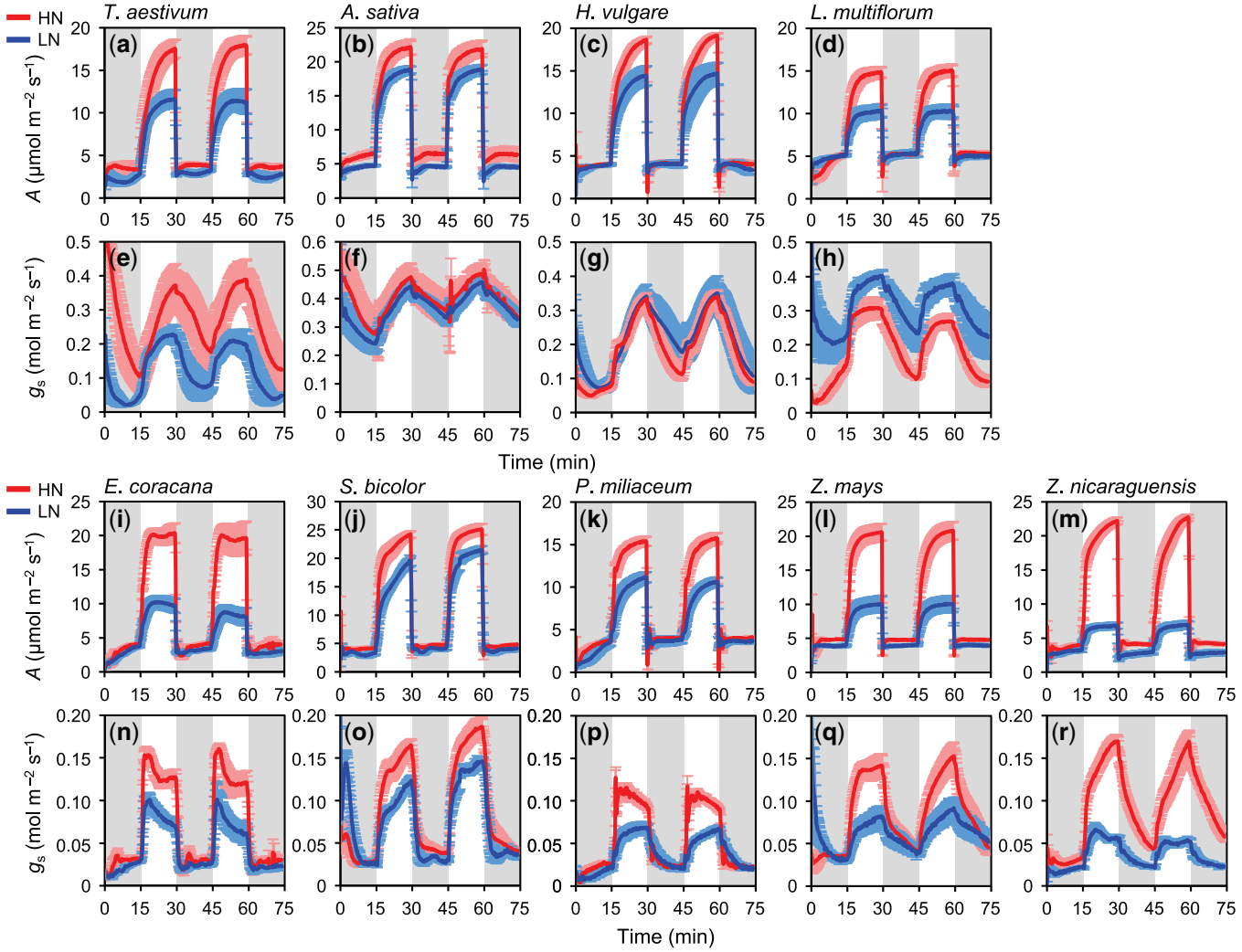

Figure 1 Dynamics of photosynthetic rate (A) and stomatal conductance (g_s) at the leaf level in the controlled fluctuating light environments in four C_3 and five C_4 species. (A–H) four C_3 and (I–R) five C_4 species. Light intensity was alternately changed between low (100 μmol m^{-2} s^{-1} PPFD, gray area) and high (1,000 μmol m^{-2} s^{-1} PPFD, white area) at 15-min intervals for a total of 75 min. Red and blue lines represent plants grown under HN and LN conditions, respectively. Data are the mean ± SE (n = 4).

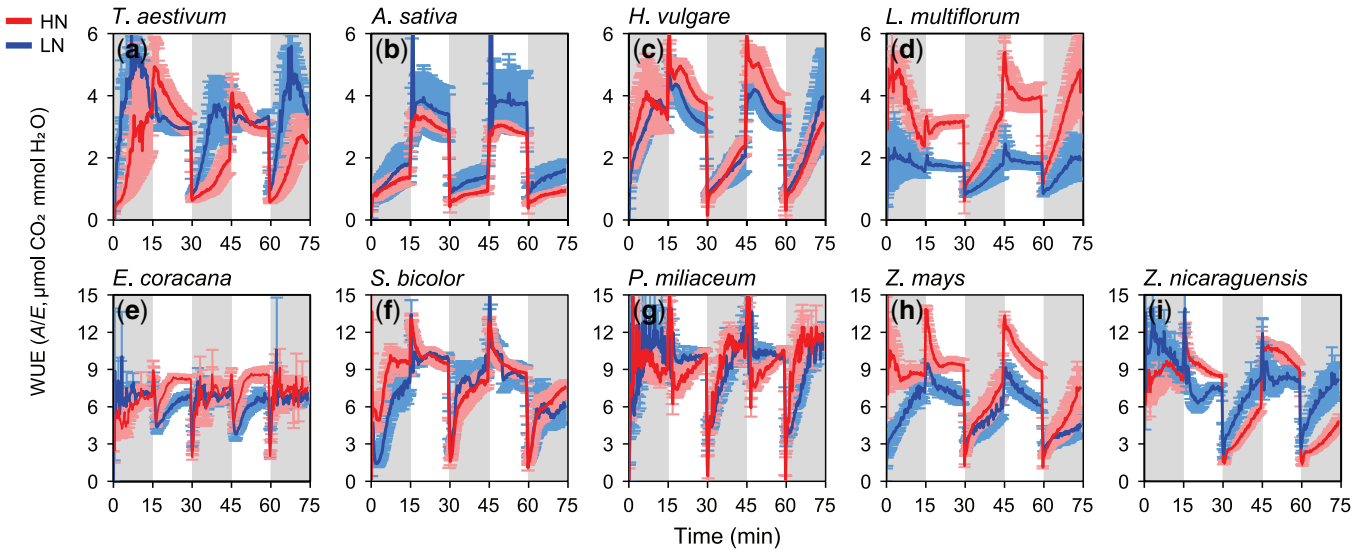

Figure 2 Dynamics of WUE in the controlled fluctuating light environments in four C_3 and five C_4 species. (A–D) C_3 species, (E–I) C_4 species. WUE was calculated as the ratio of photosynthetic rate (A) to transpiration rate (E). Light intensity was alternately changed between low (100 μmol m^{-2} s^{-1} PPFD, gray area) and high (1,000 μmol m^{-2} s^{-1} PPFD, white area) at 15-min intervals for a total of 75 min. Red and blue lines represent plants grown under HN and LN conditions, respectively. Data are the mean ± SE (n = 4).

Table 1 Mean WUE during the high light period (WUE_{HL}) and low light period (WUE_{LL}) in four C_3 species and five C_4 species grown under high and low nitrogen conditions.

Type	Species	N	WUE_{HL} (μmol CO_2 mmol H_2O^{-1})	WUE_{LL} (μmol CO_2 mmol H_2O^{-1})
C_3	*Triticum aestivum*	HN	3.54 ± 0.27	1.43 ± 0.28
		LN	3.22 ± 0.18	3.01 ± 0.52
	Avena sativa	HN	2.98 ± 0.08	0.80 ± 0.04
		LN	3.89 ± 1.01	1.28 ± 0.26
	Hordeum vulgare	HN	4.42 ± 0.24	1.69 ± 0.14
		LN	3.64 ± 0.19	1.81 ± 0.29
	Lolium multiflorum	HN	3.53 ± 0.19	2.66 ± 0.28
		LN	1.82 ± 0.13	1.38 ± 0.24
C_4	*Eleusine coracana*	HN	7.72 ± 0.30	6.80 ± 0.43
		LN	5.96 ± 0.18	6.65 ± 0.25
	Sorghum bicolor	HN	9.90 ± 0.27	6.06 ± 0.46
		LN	9.71 ± 0.13	6.26 ± 0.73
	Panicum miliaceum	HN	9.36 ± 0.29	9.49 ± 0.50
		LN	10.27 ± 0.22	8.11 ± 0.34
	Zea mays	HN	10.16 ± 0.23	5.04 ± 0.78
		LN	7.38 ± 0.40	4.23 ± 0.69
	Zea nicaraguensis	HN	9.70 ± 0.36	3.46 ± 0.16
		LN	7.99 ± 0.54	6.14 ± 0.63
	Two-way ANOVA	C_3, C_4	***	***
		N	**	NS
		C_3, C_4 × N	NS	NS

WUE_{HL} and WUE_{LL} were calculated as the ratio of photosynthetic ratio (A) to transpiration rate (E) during the high light period and the second and third low light period, respectively (Figure 2). Data are the mean ± SE (n = 4). The effects of photosynthetic types (C_3 or C_4), nitrogen conditions (HN or LN), and their interaction on the characteristics were determined by two-way ANOVA (***$P < 0.001$, **$P < 0.01$, *$P < 0.05$, NS, $P > 0.05$).

E. coracana grown under HN conditions (0.25 min and 0.36 min, respectively) and largest in *A. sativa* grown under LN conditions (3.62 min and 4.45 min respectively; Supplemental Table S1). k_{open} and k_{close} tended to be smaller in the C_4 species under HN conditions (Figure 3, A and B), whereas they varied little among the C_3 and C_4 species under LN conditions except for *E. coracana* that showed the smallest k_{open} and k_{close} (Figure 3, A–E). Overall, k_{open} was significantly correlated with k_{close} across all the species and nitrogen conditions (Figure 3E). However, *L. multiflorum* showed smaller k_{open} and larger k_{close} among the C_3 species, and *S. bicolor* showed larger k_{open} and

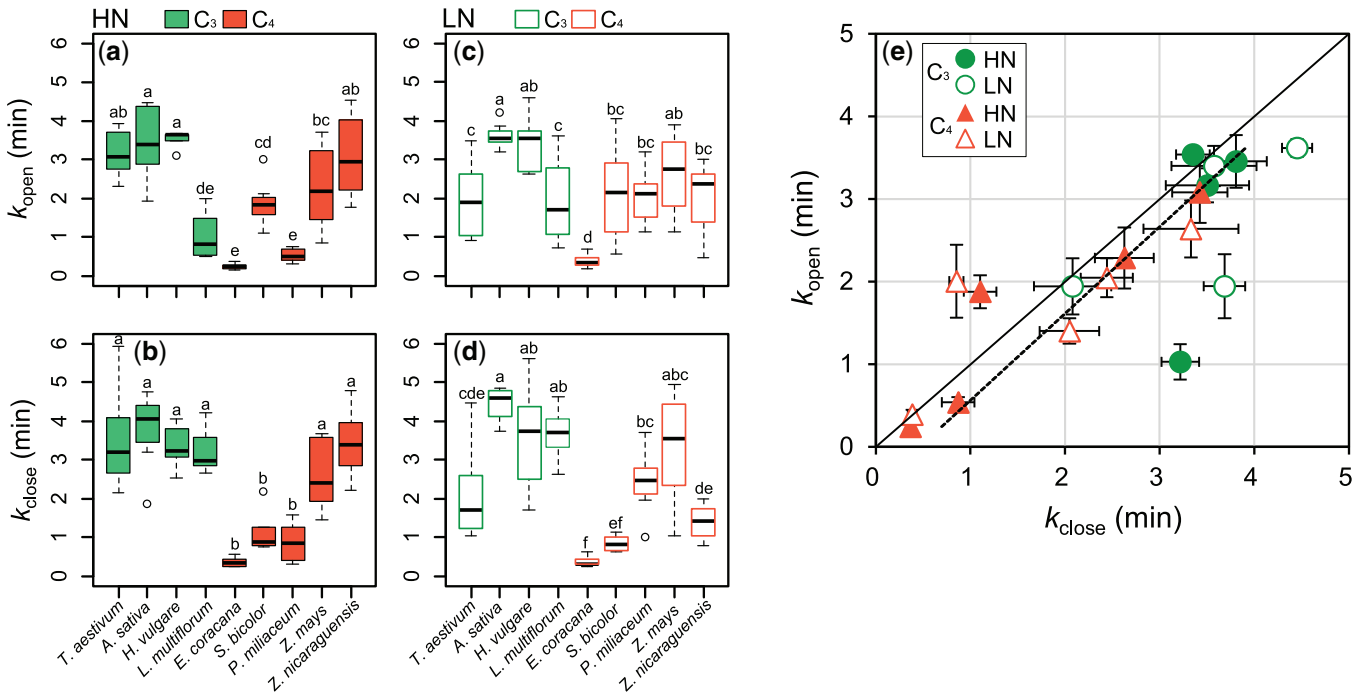

Figure 3 Time constants for stomatal opening (k_{open}) and closure (k_{close}) determined by the photosynthesis measurements in four C_3 and five C_4 species grown under HN or LN conditions. A–D, Green and orange boxes indicate C_3 and C_4 species, respectively. Boxplots represent the median (solid black line), first and third quartile (box limits), and maximum and minimum values (whiskers). Significant differences between the species were determined using ANOVA followed by Tukey's test ($P < 0.05$) and are indicated by different letters. Data are the mean ± SE ($n = 4$). *E*, In the relationship between k_{open} and k_{close}, solid and dotted lines represent regression line ($R^2 = 0.66$, $P < 0.01$) and 1:1 line, respectively.

smaller k_{close} among the C_4 species. SI_{open} and SI_{close} varied little among the C_3 and C_4 species except for *E. coracana*, which showed the highest SI_{open} and SI_{close} (Supplemental Figure S1).

Plants grown under HN showed significantly higher N_{area} and A_{max} than those grown under LN conditions. The C_3 species showed significantly higher N_{area}, lower stomatal density (SD), and longer guard cell than the C_4 species (Supplemental Table S2). We found strong correlations between physiological and morphological characteristics of stomata only for plants grown under HN conditions (Figure 4). Across the C_3 and C_4 species grown under HN conditions, k_{open} and k_{close} were significantly positively correlated with guard cell length, GL_{mean}, and significantly negatively correlated with SD_{mean} (Figure 4, A–D). On the other hand, no significant correlations were found among these traits across the C_3 and C_4 species grown under LN conditions (Figure 4, C, D, G, and H). As expected, significant negative correlation was found between SD_{mean} and GL_{mean} across the C_3 and C_4 species grown under HN and LN conditions (Supplemental Figure S2, A and B).

Whole-plant water use characteristics in fluctuating light environments

Marked differences in the dynamics of whole-plant g_s were found between the C_3 and C_4 species and nitrogen conditions (Figure 5; Supplemental Figures S3 and S4). *Triticum aestivum* and *E. coracana*, which were shown as representatives of the C_3 and C_4 species, exhibited distinct diurnal patterns of g_s. The dynamics of g_s in *E. coracana* was characterized by lower whole-plant G_{smax} and G_{smin}, more rapid increase and decrease in g_s, and consistent responses throughout the day in the fluctuating light environments at both 30-min intervals (Figure 5A) and 15-min intervals (Figure 5B). On the other hand, in *T. aestivum*, response of whole-plant g_s to fluctuating light was slower than *E. coracana*, and lower G_{smax} and higher G_{smin} were observed in the fluctuating light environments at 15-min intervals compared with those at 30-min intervals (Figure 5B). This indicated that whole-plant g_s did not reach steady state at 15-min intervals of light fluctuation. Furthermore, G_{smax} and G_{smin} changed diurnally in *T. aestivum*, whereas they were stable in *E. coracana*, and other C_3 and C_4 species showed trends similar to *T. aestivum* (Supplemental Figure S3) and *E. coracana* (Supplemental Figure S4), respectively.

The C_4 species showed significantly smaller whole-plant k_{open} and k_{close} than the C_3 species (Figure 6; Supplemental Table S3). Whole-plant k_{open} and k_{close} changed diurnally in the C_3 species (Figure 6, A, B, E, and F). Among the C_3 species, *L. multiflorum* grown under HN conditions showed the smallest k_{open} and k_{close}. Whole-plant k_{open} and k_{close} were less than 1 min (Supplemental Table S3) and stable throughout the day for all the C_4 species (Figure 6, C, D, G, and H).

Whole-plant k_{open} was significantly correlated with whole-plant k_{close} across all the species and nitrogen conditions

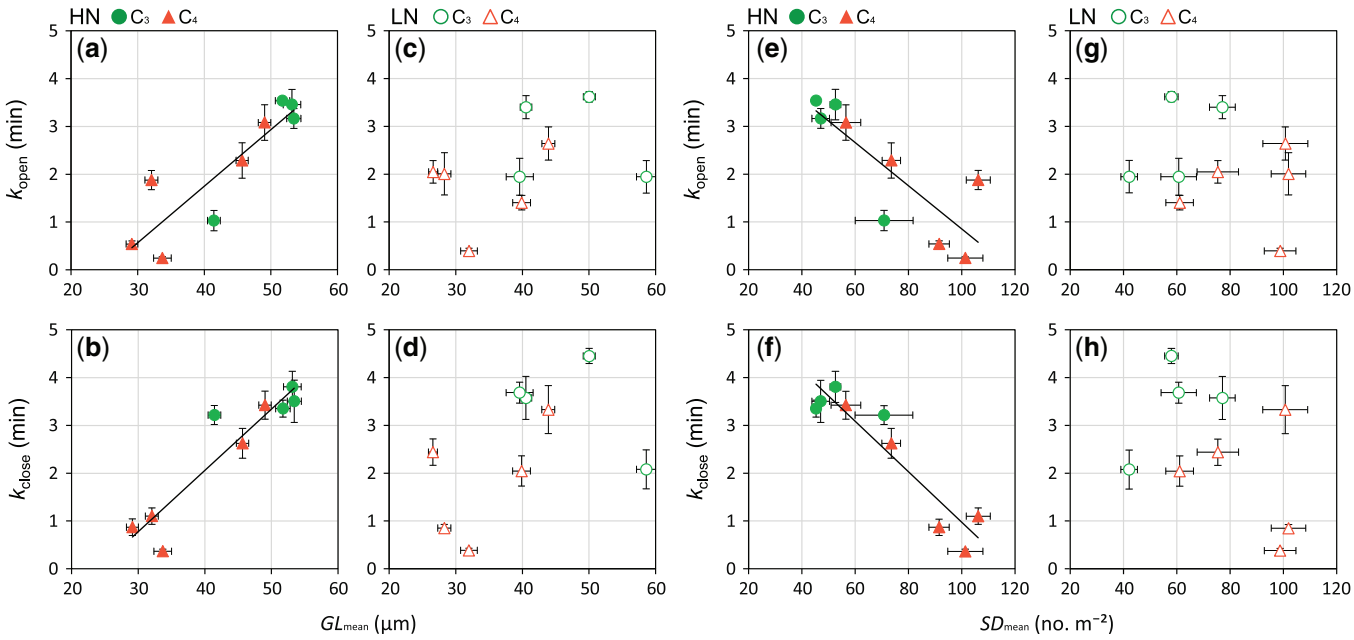

Figure 4 Relationship between time constants for stomatal opening (k_{open}) or closure (k_{close}) and mean GL_{mean} or mean SD_{mean} in four C_3 and five C_4 species grown under HN or LN conditions. (A, B, E, and F) HN condition and (C, D, G, and H) LN condition. Green and orange symbols indicate C_3 and C_4 species, respectively, and filled and open symbols indicate plants grown under HN and LN conditions, respectively. Regression lines are shown for all C_3 and C_4 species. Values of R^2 are (A) 0.79 ($P < 0.01$), (B) 0.86 ($P < 0.01$), (E) 0.68 ($P < 0.01$), (F) 0.87 ($P < 0.01$). Data are the mean ± SE ($n = 4$).

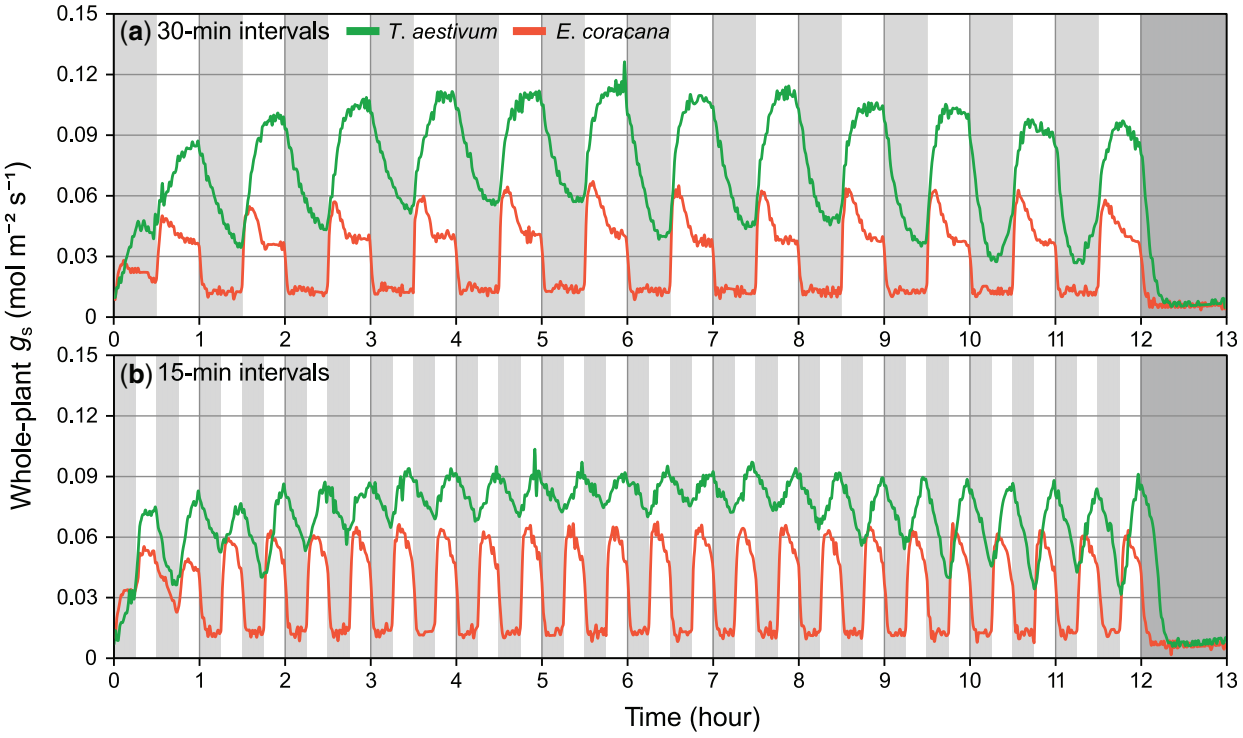

Figure 5 Dynamics of the whole-plant stomatal conductance (g_s) in the controlled fluctuating light environments in *T. aestivum* and *E. coracana*. Light intensity was alternately changed between low (80 μmol m^{-2} s^{-1} PPFD at 30-cm above the pot surface, gray area) and high (300 μmol m^{-2} s^{-1} PPFD at 30 cm above the pot surface, white area) at 30-min intervals (A) and 15-min intervals (B) for a total of 12 h. Light was turned off from after the measurements (dark gray area). Green and orange lines represent *T. aestivum* (C_3 species) and *E. coracana* (C_4 species), respectively. Data are the mean of four pot plants on the balance.

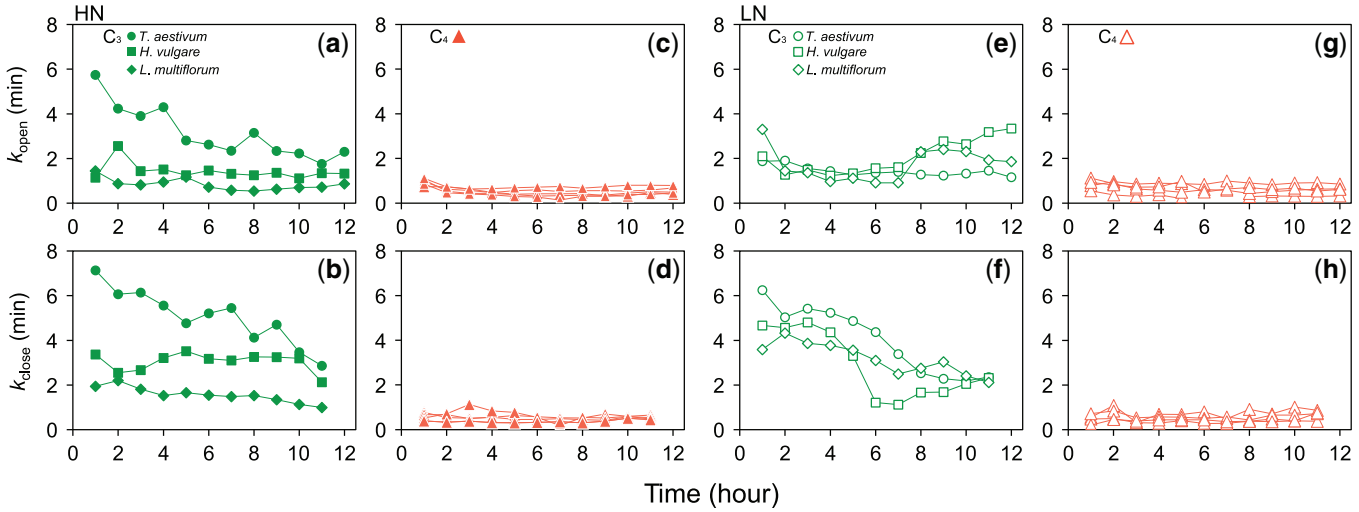

Figure 6 Diurnal changes in time constants for stomatal opening (k_{open}) or closure (k_{close}) calculated from the whole-plant stomatal conductance (g_s) in three C_3 and five C_4 species grown under HN or LN conditions. (A, B, C, and D) HN condition and (E, F, G, and H) LN condition. The results obtained in fluctuating light environments at 30-min intervals are shown. Data for *A. sativa* grown under HN and LN and *Z. nicaraguensis* grown under LN were not shown since we could not fit the temporal responses of g_s to the equations due to small differences in G_{smax} and G_{smin} (Supplemental Figures S3, C and S4I). Data are calculated from four pot plants on the balance.

(Supplemental Figure S5A). Whole-plant k_{open} and k_{close} were comparable in the C_4 species, whereas k_{close} was significantly larger than k_{open} in the C_3 species (Supplemental Table S3). Comparing the leaf-level and whole-plant stomatal characteristics obtained at moderate change (80–300 μmol m^{-2} s^{-1}) and large change (100–1,000 μmol m^{-2} s^{-1}) in light intensity, no significant correlations were observed between whole-plant k_{open} or k_{close} and leaf-level k_{open} or k_{close} (Supplemental Figure S5, B and C).

Simulation of the dynamic photosynthesis model

We can see how changes in light intensity and g_s could affect the photosynthetic rate through changes in A_j and C_m for C_3 species and C_{bs} for C_4 species (Supplemental Figure S6). In both C_3 and C_4 photosynthesis models, the CO_2 assimilation rate is limited by g_s at high light intensity (Supplemental Figure S6, A and C), whereas it was limited by the RuBP regeneration rate at low light intensity (Supplemental Figure S6, B and D).

The dynamic photosynthesis model which related g_s dynamics and the CO_2 assimilation models could accurately predict the dynamics of *A*, *E*, and WUE calculated as *A*/*E* in the fluctuating light environments in both *T. aestivum* (C_3 species) and *E. coracana* (C_4 species; Figure 7). Although *E.* coracana might show overshoot of stomatal opening (Figure 7E), which resulted in the lower WUE (Figure 7H) at the beginning of the high light period, observed and simulated values were generally consistent. These consistencies indicate that effect of changes in k_{open} and k_{close} on *A*, *E*, and WUE can be accurately simulated in these species.

Based on the present results (Figure 3E) and previous studies (Vico et al., 2011; Israel et al., 2021) showing that k_{open} and k_{close} are not necessarily consistent with each other, we simulated the effect of both independent and simultaneous changes in k_{open} and k_{close} on *A*, *E*, and WUE. In *T. aestivum* with intrinsic large k_{open} and k_{close}, by decreasing k_{open}, i.e. accelerating stomatal opening, A_{total} and E_{total} increased by 7.1% and 14.5%, respectively, resulting in 6.4% decrease in WUE_{total} (Figure 8A). On the other hand, decreasing k_{close}, i.e. accelerating stomatal closure, little affected A_{total} (0.6% decrease) but decreased E_{total} by 14.5%, resulting in 16.2% increase in WUE_{total} (Figure 8B). This is because accelerating stomatal opening (Supplemental Figure S7A) only slightly increased *A* (Supplemental Figure S7B) but more substantially increased *E* (Supplemental Figure S7C), resulting in decreased WUE during the high light period (Supplemental Figure S7D). Meanwhile, accelerating stomatal closure (Supplemental Figure S7E) little increased *A* (Supplemental Figure S7F) but decreased *E* and increased WUE during the low light period (Supplemental Figure S7, G and H). When k_{open} and k_{close} were decreased simultaneously, A_{total} increased by 6.5%, whereas E_{total} did not change, resulting in only 6.5% increase in WUE_{total} (Figure 8C).

In the case of *E. coracana* with intrinsic small k_{open} and k_{close}, increasing k_{open}, i.e. decelerating stomatal opening, largely decreased A_{total} (22.5% decrease) and E_{total} (21.8%), resulting in slight decrease in WUE_{total} (0.8% decrease) (Figure 8D). Increasing k_{open}, i.e. decelerating stomatal closure, affected A_{total} little but increased E_{total} by 22%, resulting in 17% decrease in WUE_{total} (Figure 8E). This is because decelerating stomatal opening (Supplemental Figure S7I), decreased *A* and *E* (Supplemental Figure S7, J and K) but affected WUE little during the high light period (Supplemental Figure S7I). Meanwhile, decelerating stomatal closure (Supplemental Figure S7M) affected *A* little (Supplemental Figure S7N) but increased *E* and decreased WUE during the low light period (Supplemental Figure S7, O and P). When k_{open}

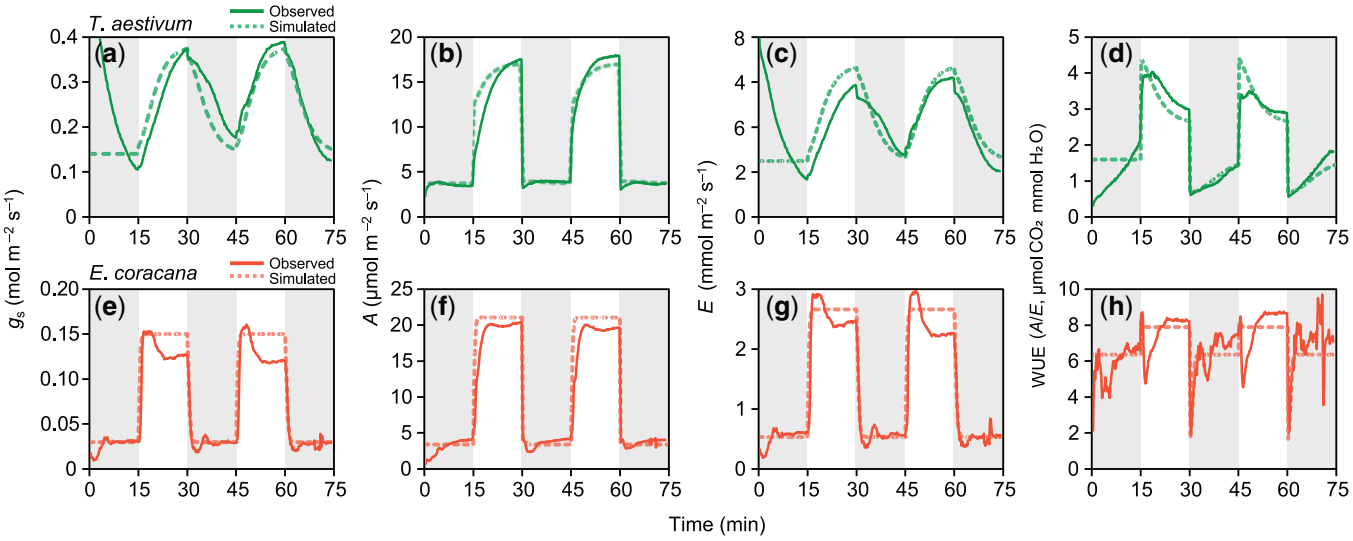

Figure 7 Observed and simulated photosynthetic characteristics (stomatal conductance (g_s), photosynthetic rate (A), transpiration rate (E), and WUE (A/E) in the controlled fluctuating light environments in *T. aestivum* and *E. coracana* grown under HN conditions. (A and E) Stomatal conductance (g_s), (B, F) photosynthetic rate (A), (C, G) transpiration rate (E), and (D and H) WUE (A/E) are shown. Solid and broken lines represent observed and simulated values, respectively.

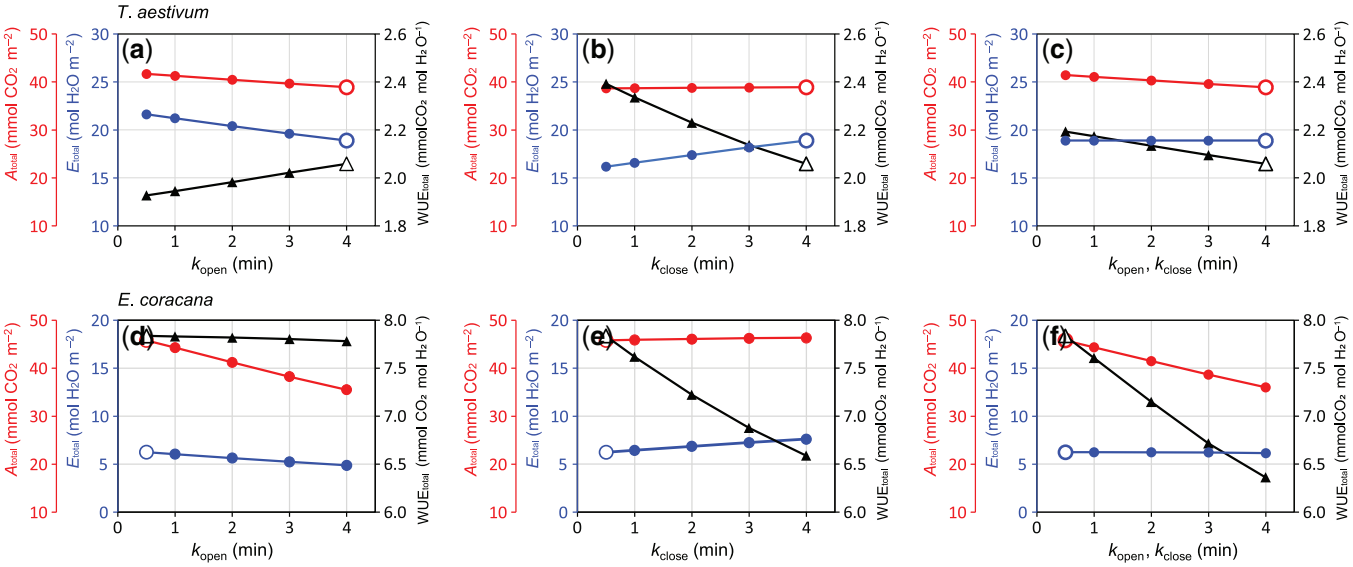

Figure 8 Effects of changes in time constants for stomatal opening (k_{open}) and closure (k_{close}) on total photosynthesis (A_{total}), total transpiration (E_{total}), and total WUE_{total} during the 75 min fluctuating light period. In *T. aestivum*, k_{close} was kept constant at 4 min and k_{open} was varied from 4 to 0.5 (A), or k_{open} was kept constant at 4 min and k_{close} was varied from 4 to 0.5 (B). In *E. coracana*, k_{close} was kept constant at 0.5 min and k_{open} was varied from 0.5 to 4 (D), or k_{open} was kept constant at 0.5 min and k_{close} was varied from 0.5 to 4 (E). k_{open} and k_{close} were simultaneously varied from 0.5 to 4 and 4 to 0.5 in *T. aestivum* (C) and *E. coracana* (F), respectively. For each combination of k_{open} and k_{close}, A_{total}, E_{total} and WUE_{total} were simulated by the dynamic photosynthesis model. Open and filled symbols represent the initial and simulated values, respectively.

and k_{close} were increased simultaneously, E_{total} little affected, whereas A_{total} decreased by 21.3%, resulting in only 20% decrease in WUE_{total} (Figure 8E).

Although there were no significant correlations between WUE_{HL} and k_{open} (Supplemental Figure S8, A and B), there was significant negative correlation between WUE_{LL} and k_{close} among the C_3 and C_4 species grown under HN conditions consistent with the prediction (Supplemental Figure S8C).

Discussion

Rapid stomatal closure contributes to higher WUE in major C4 crops

In the present study, we found that the C_4 crops exhibited substantially more rapid stomatal opening and closure than the C_3 crops in the fluctuating light environments. Such rapid responses could be partly explained by the differences in stomatal morphology and density observed across all the species. The model simulation suggests that greater CO_2

assimilation and higher WUE of the C_4 species over the growth period are achieved by rapid stomatal opening and closure, respectively. These results further suggest that rapid stomatal closure could improve WUE of the C_3 species, which may be a potential target for genetic engineering of C_3 Poaceae crops.

Stomatal morphology and plant nutrient status influenced stomatal kinetics

McAusland et al. (2016) reported marked differences in k_{open} and k_{close} among 13 important crops including the crops used in the present study. In that study, it was shown that dicotyledonous crops with elliptical-shaped guard cells showed larger k_{open} (6.9–23.4 min), whereas Poaceae crops showed smaller k_{open} (0.9–4.4 min) and k_{close} (0.9–4.1 min), and rapid stomatal response was attributed to the dumbbell-shaped guard cells. Our results further revealed that the C_4 species showed more rapid stomatal opening and closure at the leaf level even among Poaceae family with dumbbell-shaped guard cells (Figure 1), as indicated by the significantly smaller leaf-level k_{open} and k_{close} (Supplemental Table S1). Consistent with previous reports showing positive correlations between k_{open} and k_{close} among various banana varieties (Eyland et al., 2021) and among a wide range of plant species from graminoid to woody gymnosperm (Vico et al., 2011), the present study found k_{open} and k_{close} were closely related in Poaceae species (Figure 3E), suggesting the presence of common factors determining the potential of stomatal opening and closure regardless of plant functional types.

Morphological analysis suggests that factors affecting k_{open} and k_{close} are GL or SD, which is supported by the strong positive relationship between GL_{mean}, k_{open}, and k_{close} across the C_3 and C_4 species grown under HN conditions (Figure 4, A, B, E, and F; Supplemental Table S2). It seems reasonable that smaller guard cells showed rapid stomatal response due to greater surface area to volume ratio and less requirements of solutes, which could cause faster expansion and contraction of guard cells by faster water influx and efflux, respectively (Drake et al., 2013; Elliott-Kingston et al., 2016). On the other hand, Zhang et al. (2019) found negative correlation between k_{open} and stomatal size among sixteen *Oryza* genotypes, indicating that the present finding may be applicable to upland crops but not to lowland crops with unlimited access to water. Recently, it is reported that the genetic variation in *OsNHX1*, Na^+/H^+ tonoplastic antiporter, is strongly associated with the time required for stomatal closure in *O. sativa* especially under drought stress (Qu et al., 2020), indicating the importance of considering genetic variation in stomatal physiology. Another important finding was that no significant relationship was found between k_{open}, k_{close}, and stomatal morphology under LN conditions (Figure 4, C, D, G, and H). Although no significant effect of nitrogen conditions on stomatal morphology was statistically confirmed (Supplemental Table S2), it is likely that guard cell metabolism was modulated by the changes in ion, protein, and starch content under LN conditions (Lawson and Matthews, 2020). Recent studies have also shown that subsidiary cells facilitated guard cell functions through the translocation of H^+-ATPase, by serving as ion source and sink and providing mechanical strength (Higaki et al., 2014; Raissig et al., 2017; Gray et al., 2020). In these regards, single-cell metabolomics and ultrastructural observations in guard cells and subsidiary cells will uncover the factors determining stomatal kinetics as affected by soil nitrogen conditions, which could further lead to the proposal of crop-specific fertilization and water-saving managements. Interestingly, *Z. mays* and its wild relative *Z. nicaraguensis* with longer GL_{mean} showed slower stomatal responses among the C_4 species. Although these two species are diploid (Trtikova et al., 2017), it is reported that ploidy level correlates with stomatal size (Beaulieu et al., 2008; Lundgren et al., 2019). To understand the stomatal diversity among C_3 and C_4 Poaceae crops, it is essential to consider the process of domestication from phylogenetic and ecophysiological perspectives.

We demonstrated that the observed rapid stomatal opening and closure could contribute to the higher WUE in the C_4 Poaceae crops during light transitions (Figure 2 and Table 1). Lawson and Vialet-Chabrand (2019) also theoretically evaluated potential water loss due to slower stomatal closure during shade fleck, indicating the importance of rapid stomatal closure for the improvement of WUE (Lawson and Blatt, 2014). Taken together with the previous studies, the present results suggest that leaf-level rapid stomatal closure of the C_4 crops is a potential target for the improvement of C_3 crop drought tolerance.

C_4 species exhibited rapid stomatal responses even at the whole-plant level

We have established the system to evaluate whole-plant g_s which reflects species-specific leaf arrangement and light use efficiency (Supplemental Figure S9), which also enables to evaluate diurnal patterns of water use. The system revealed that the C_4 species exhibit more rapid stomatal opening and closure than the C_3 species at the whole-plant level (Figure 5; Supplemental Figures S4 and S5). It is notable that *Z. mays* and *Z. nicaraguensis* showed comparable whole-plant k_{open} and k_{close} with other C_4 species (Figure 6; Supplemental Table S3) despite larger leaf-level k_{open} and k_{close} (Supplemental Figure S5, B and C), suggesting that these species could respond rapidly to moderate changes in light intensity (300 μmol m^{-2} s^{-1}) which are more frequently observed in the field environments (Miyashita et al., 2012). Meanwhile, all the C_3 species showed slower stomatal responses even at the whole-plant level (Supplemental Figure S5, B and C), suggesting that the C_3 species would exhibit slower stomatal response even in the field environments. Taken together, k_{open} and k_{close} could be dependent on the magnitude of light intensity change and guard cell

size, which determine the amount of substances required for stomatal opening and closure, in major Poaceae crops.

Interestingly, some C_3 species showed diurnal changes in whole-plant k_{open} and k_{close} (Figure 6), suggesting that diurnal changes in potassium ion and sucrose contents affected stomatal responses in those C_3 species (Talbott and Zeiger, 1998; Daloso et al., 2016). We have previously argued that sugar accumulation could cause photosynthetic downregulation through a deceleration of stomatal opening and decreased maximum g_s (Sugiura et al., 2019, 2020). Therefore, it is likely that stable stomatal responses in the C_4 species could be attributed to lower accumulation of sugars and starch, which was achieved by higher sucrose export rate in C_4 plants compared with C_3 plants (Gallaher et al., 1975; Grodzinski et al., 1998).

A major limitation of the present system is that it cannot be applied to field-grown crops. It is essential to develop a new technique to understand stand-level water use characteristics and to solve the above issues in the field.

Contribution of rapid stomatal responses predicted by the dynamic photosynthesis model

Although the structure of the present model is quite simple, with a constant relationship between g_{sc} and g_{mc}, it successfully simulated the changes in g_s, A, and WUE in the controlled fluctuating light environments (Figure 7). This demonstrates the reliability of the model structure (Supplemental Figure S6) and validity of the parameter values used for both *T. aestivum* and *E. coracana* (Table 2). Therefore, we can assume that the model can predict dynamics of g_s, A, and WUE in plants with altered k_{open} and k_{close} with a certain accuracy (Supplemental Figure S7). In accordance with previous studies (Vico et al., 2011; Israel et al., 2021), k_{open} and k_{close} are not necessarily consistent with each other (Figure 3E), and k_{open} and k_{close} are not determined by stomatal morphology under LN conditions (Figure 4). These findings imply that different mechanisms could be involved in the regulation of stomatal opening and closure and motivated us to evaluate the effect of independent changes in k_{open} and k_{close} on A, E, and WUE. Israel et al. (2021) indicated a possible involvement of rate of potassium influx to guard cells with stomatal opening. Further investigation is required to uncover what physiological mechanisms are involved in stomatal closure.

Table 2 Parameter values used for the C_3 and C_4 photosynthesis models

Parameter	Unit	C_3	C_4
G_{smax}	mol m^{-2} s^{-1}	0.38	0.16
r_{open}	mol m^{-2} s^{-1}	0.14	0.03
k_{open}	min	3.2	0.25
G_{smin}	mol m^{-2} s^{-1}	0.14	0.03
r_{close}	mol m^{-2} s^{-1}	0.38	0.16
k_{close}	min	3.5	0.36
V_{cmax}	μmol m^{-2} s^{-1}	78.45	40
Γ^*	μmol mol^{-1}	37.74	10
K_c	μmol mol^{-1}	488	650
K_o	μmol mol^{-1}	343	450
C_a	μmol mol^{-1}	400	400
O	mmol mol^{-1}	200	200
J_{max}	μmol m^{-2} s^{-1}	145.10	120
R_d	μmol m^{-2} s^{-1}	1.35	1
φ_r	–	0.3	0.2
θ_r	–	0.95	0.8
V_{pmax}	μmol m^{-2} s^{-1}	–	120
V_{pr}	μmol m^{-2} s^{-1}	–	80
K_p	μmol mol^{-1}	–	80
g_{bs}	mol m^{-2} s^{-1}	–	0.003

For C_3 photosynthesis model, V_{cmax}, J_{max}, and R_d were obtained from the measurement of CO_2 response curves of *T. aestivum* in the present study. As for the other parameters such as Γ^*, K_c, and K_o, values of *T. aestivum* obtained in previous study were used (Silva-Pérez et al., 2017). For C_4 photosynthesis model, other than stomatal kinetics of *E. coracana*, typical parameter values were used following previous studies (von Caemmerer, 2000; Vico and Porporato, 2008; Osborne and Sack, 2012).

The model simulation indicates that acceleration of stomatal opening would cause a large increase in water loss with little increase in CO_2 assimilation, resulting in a large decrease in WUE in the C_3 species *T. aestivum* with intrinsically large k_{open} (Figure 8A). This suggests that further acceleration of stomatal opening would be less beneficial for C_3 Poaceae crops considering that all the C_3 Poaceae crops showed k_{open} of <5 min, which are already much faster than other dicotyledonous crops. The importance of rapid stomatal opening for the improvement of photosynthetic induction is often discussed using dark-acclimated leaves with possibly large k_{open}. However, since light intensity gradually increases from dawn under field conditions, it would be appropriate to use low or high light-acclimated leaves to discuss the stomatal limitation of photosynthesis under field conditions.

Our simulation clearly indicated that rapid stomatal closure would reduce unnecessary water loss and improve WUE without decreasing A_{total} in C_3 species even within the range observed among the focal species (Figure 8B), but the advantage would be partially lost by the simultaneous acceleration of stomatal opening (Figure 8C). This idea is supported by the observation that *T. aestivum* grown under LN conditions with smaller k_{close} showed higher WUE compared with *T. aestivum* grown under HN conditions during the low light period (Figure 2A). The observed negative correlation between WUE_{LL} and k_{close} among the C_3 and C_4 species also support this idea (Supplemental Figure S8C). It is also reported that cultivars with rapid stomatal closure show higher WUE in *O. sativa* (Qu et al., 2016, 2020), *Beta vulgaris* (Barratt et al., 2021), and *Musa* spp (Eyland et al., 2021). Considering that agricultural water accounts for 70% of the world freshwater use (Rosegrant et al., 2009), the predicted 14.5% reduction in E_{total} could make a substantial contribution to reducing agricultural water use for major upland crops such as wheat, barley, and maize. Although the evaluation of k_{open} and k_{close} is laborious as shown in the present study, measurement of *SD* and *GL* may facilitate efficient selection of varieties with high WUE. Despite showing similar GL and SD to C_3 and C_4 Poaceae species, C_3 dicotyledonous crops with elliptical-shaped guard cells are reported to exhibit quite slow stomatal closure compared with the

Poaceae species (McAusland et al., 2016). A recent study demonstrated that guard cell-specific expression of K^+ channel dramatically accelerated both stomatal opening and closure in Arabidopsis, resulting in the improved WUE and growth (Papanatsiou et al., 2019). These suggest that there is much room for improving WUE by accelerating stomatal closure in those C_3 dicots, which could further contribute to improving plant productivity under drought conditions. Although our model could predict A and g_s with fewer parameters compared with previous dynamic photosynthesis models, incorporating metabolomic (Wang et al., 2021) and temperature-dependent biochemical models (Hikosaka et al., 2006; Yamori et al., 2012; Scafaro et al., 2011) will further clarify limiting processes of photosynthesis in fluctuating environments.

Why do C_4 species show a rapid stomatal response?

The simulation results demonstrated the hypothesis that higher WUE was attributed not only to higher A and lower g_s but also to rapid stomatal opening and closure minimizing unnecessary water loss in the C_4 Poaceae crops (Figure 8, D–F). There is no doubt that these rapid stomatal responses enable C_4 plants to adapt to drought conditions along with the CO_2 concentrating mechanism. By comparing stomatal characteristics among C_4 plants along precipitation and temperature gradients, it is possible to test the hypothesis that C_4 species growing in more arid region would exhibit more rapid stomatal closure. In this context, it is also hypothesized that NAD-malic enzyme (NAD-ME) C_4 species would show the most rapid stomatal response and highest drought tolerance among three major C_4 subtypes (NAD-ME, NADP-malic enzyme (NADP-ME), and PEP carboxykinase (PCK)) since the abundance of NAD-ME C_4 species increases with the decrease in annual precipitation (Henderson et al., 1994; Schulze et al., 1996). This hypothesis deserves to be tested, since the sole NAD-ME type C_4 crop, *E. coracana* with higher drought tolerance (Talwar et al., 2020) showed the smallest k_{open} and k_{close} regardless of nitrogen conditions in the present study. Another important issue is whether C_4 dicots exhibit rapid stomatal opening and closure like the C_4 Poaceae species. Although C_4 dicots such as *Flaveria* and *Amaranthus* with elliptical-shaped guard cells are known to exhibit higher leaf-level WUE at the saturating light intensity (Vogan and Sage, 2011; Tsutsumi et al., 2017), the above hypothesis has not been tested yet. The present simple dynamic photosynthesis model that can accurately evaluate CO_2 assimilation, water consumption, and WUE will be useful to address which parameters are optimized thorough the stomatal behavior depending on drought, soil nutrients, and atmospheric CO_2 concentration in C_4 plants. For this purpose, the accuracy of the model predictions should be tested by simulating natural light fluctuation throughout day period in the gas exchange system and comparing predicted and observed A, g_s, and WUE.

Conclusions

In the present study, we have quantified stomatal kinetics in four C_3 and five C_4 Poaceae species in controlled fluctuating light environments. We have developed a system enabling the continuous measurement of whole-plant water use throughout a day. The major C_4 crops exhibited more rapid stomatal opening and closure than the C_3 crops at the leaf and the whole-plant levels, which contributed to higher WUE of the C_4 crops. In particular, rapid stomatal closure enhanced WUE by reducing unnecessary water loss during low light period. Morphological analysis indicated that smaller *GL* and higher *SD* could be attributed to the faster stomatal kinetics for plants grown at HN conditions. These results are supported by the sensitivity analysis by our dynamic photosynthesis model that incorporates the C_3 and C_4 photosynthesis models with stomatal dynamics. The present results indicate that acceleration of stomatal closure of major C_3 crops to the level of major C_4 crops is a potential breeding target for the realization of water-saving agriculture.

Materials and methods

Plant material and growth conditions

We selected a total of nine C_3 and C_4 species, all belonging to the Poaceae family and regarded as major cereal crops in the world except for *Zea nicaraguensis*. For C_3 species, we used wheat (*Triticum aestivum* cv. Norin 61), oat (*Avena sativa* cv. Tachiibuki), barley (*Hordeum vulgare* cv. Shunrai), and Italian ryegrass (*Lolium multiflorum* cv. Waseaoba). For C_4 species, we used finger millet (*Eleusine coracana* cv. Yukijirushi-kei), sorghum (*Sorghum bicolor* cv. Tsuchitaro), millet (*Panicum miliaceum*), maize (*Zea mays* cv. Honey bantam), and its wild relative *Zea nicaraguensis* (CIMMYT 13451).

For each species, four plants were grown in a growth room at 27°C, 40% relative humidity, and a 12/12-h photoperiod. Light was provided by white light LED source (LD93-D, GOODGOODs, Osaka, Japan), which provide a photosynthetically active photon flux density (PPFD) of 250, 300, 400 μmol m^{-2} s^{-1} at 0 cm, 30 cm, and 60 cm above the pot surface, respectively.

Seeds were sown and germinated in 500-mL plastic pots filled with peat-based compost (Natural Applied Sciences, Gifu, Japan). Plants were grown with or without nitrogen fertilizer. For plants grown under HN condition, 0.4 g of a slow-released nitrogen fertilizer containing 42% nitrogen (LP40, JCAM Agri, Tokyo, Japan), and 0.8 g of an inorganic fertilizer containing 20% of K_2O and P_2O_5 (PK40, Onoda chemical, Tokyo, Japan) were mixed with the soil, and 50 mL of 1/500 strength nutrient solution (HYPONeX, N/P/K, 6:10:5, Hyponex Japan, Osaka, Japan) was added every 2 or 3 d. For plants grown without nitrogen fertilizer (LN), only 0.8 g of the inorganic fertilizer was mixed with the soil. Pots were placed in the same container for each species and nitrogen condition, and they were watered regularly.

Continuous measurement of whole-plant water use in fluctuating light environments

Plants were grown for different period since the growth rate was different among species dependent on seed size and nitrogen conditions. For C_3 species under HN conditions, *T. aestivum*, *A. sativa*, *H. vulgare*, and *L. multiflorum* were grown for 45, 35, 45, and 45 d, respectively. For C_4 species under HN conditions, *E. coracana*, *S. bicolor*, *P. miliaceum*, *Z. mays*, and *Z. nicaraguensis* were grown for 45, 40, 40, 40, and 50 d, respectively. For C_3 species under LN conditions, *T. aestivum*, *A. sativa*, *H. vulgare*, and *L. multiflorum* were grown for 45, 35, 50, and 60 d, respectively. For C_4 species under LN conditions, *E. coracana*, *S. bicolor*, *P. miliaceum*, *Z. mays*, and *Z. nicaraguensis* were grown for 45, 45, 55, 50, and 65 d, respectively.

We have developed a system to measure whole-plant water use continuously (Supplemental Figure S9). On two consecutive days, whole-plant water consumption was evaluated in controlled fluctuating light environments in the growth room, where light intensity was alternately changed between low (30% of maximum light intensity, 80 μmol m^{-2} s^{-1} PPFD at 30 cm above the pot surface) and high (300 μmol m^{-2} s^{-1} PPFD at 30 cm above the pot surface) at 30-min intervals on the first day and 15-min intervals on the second day. For each species, the soil surface was covered with a plastic sheet to prevent soil evaporation, and four pots were placed on a Bluetooth communication electronic balance with the minimum unit of 0.01 g (RJ-3200, Shinko Denshi, Tokyo, Japan) at the beginning of the light period. The balance was connected to a recording device (ZenPad 8.0, ASUS corporation, Taiwan) with an automatic logging application (Weight Data Logger, Digital Workshop Kinos, Tokyo, Japan), which were developed for the present study, and water consumption rate of the four pot plants (WC_4, g s^{-1}) was recorded at 1-min intervals. During the pot weight measurement, PPFD (S-LIA-M003, Onset Computer Corporation, Bourne, MA, USA), air temperature (T_a, °C), and relative humidity (RH, %; S-THB-M002, Onset Computer Corporation) were also measured at 1-min intervals and recorded on a data logger (HOBO Micro Station, Onset Computer Corporation).

After leaf area measurement on the third day (see below), whole-plant transpiration rate (E, mol m^{-2} s^{-1}) and g_s (mol m^{-2} s^{-1}) were calculated from leaf area (LA_4, m^2) and WC_4 as follows:

$$\text{Whole} - \text{plant } E = \frac{WC_4/18}{LA_4} \quad (1)$$

$$\text{Whole} - \text{plant } g_s = \frac{\text{whole} - \text{plant } E}{\text{VPD}/101.3} \quad (2)$$

where 18 is the molecular weight of water, and VPD is further calculated from T_a and RH assuming leaf temperature (T_L, °C) is equal to T_a as follows:

$$\text{VPD} = 0.611 \times e^{\left(\frac{17.3*Ta}{Ta+237}\right)} \times \left(1 - \frac{\text{RH}}{100}\right) \quad (3)$$

We checked the validity of the assumption that T_L was almost equal to T_a by direct measurements of T_a and T_L, showing that the difference between T_a and T_L were less than 2°C and 1°C in *T. aestivum* and *E. coracana*, respectively (Supplemental Figure S10). Briefly, T type thermocouples were attached to the abaxial side of the youngest fully expanded leaves, and T_L was recorded at 1-min intervals and recorded on a data logger (Ondotori TR-55i, T&D, Nagano, Japan) at 30-min intervals of light fluctuation.

In our system, whole-plant E changed with time in species-specific manners even under steady light intensity (see "Results"), suggesting that leaves were coupled to the atmosphere if not fully (McNaughton and Jarvis 1991). Therefore, we concluded that our simplified calculation was effective to capture the species-specific patterns in the whole-plant g_s in responses to the changing light intensity.

Leaf gas exchange measurement in fluctuating light environments

On the third day after the measurements of whole-plant g_s, the youngest fully expanded leaves were used for photosynthesis measurements using a portable gas exchange system (LI-6800, LI-COR Biosciences, Lincoln, NE, USA). The measurement started just after plants were transferred to a measurement room. The leaf chamber was maintained at 400 μmol mol^{-1} CO_2 concentration (C_a), a leaf temperature of 25°C, and RH of 50%. To evaluate potential A and g_s in controlled fluctuating light environments (McAusland et al., 2016), light intensity was alternately changed between low (100 μmol m^{-2} s^{-1} PPFD) and high (1,000 μmol m^{-2} s^{-1} PPFD) at 15-min intervals for a total of 75 min, and A and g_s were recorded every 10 s. WUE was calculated as the ratio of A to E, and mean WUE during the high light period (WUE_{HL}) and the second and third low light periods (WUE_{LL}) were obtained. Maximum A during the measurements was defined as A_{max}.

Measurements of SD and GL

After the photosynthesis measurements, nail vanish peels were taken from adaxial and abaxial sides of the same leaves. Images were obtained by light microscopy (BX41, Olympus, Tokyo, Japan). SD and *GL* were determined from three fields of view (1.85 or 0.29 mm^2 in field area) on adaxial and abaxial surfaces using ImageJ (Schneider et al., 2012). Mean SD (SD_{mean}) and GL_{mean} were calculated as the mean values of SD and GL on adaxial and abaxial sides of the leaves, respectively.

Leaf area measurement and CN analysis

For each plant, all green leaf blades were dissected and placed between a transparent acrylic plate and a white

acrylic plate. Photos were taken using smartphone camera application with skew correction function (Office Lens, Microsoft Corp, Redmond, USA), and green leaf area was determined using the ImageJ. After leaf area measurements, each plant was divided into the leaf used for photosynthesis measurement, rest of the leaves, leaf sheath, and roots. They were oven-dried for >48 h at 80°C and weighed to determine dry mass. Leaves used for photosynthesis measurement were finely ground using a mill (TissueLyser II, Retsch, Haan, Germany), and leaf nitrogen content per mass (N_{mass}, g N g^{-1}) was determined with a CN analyzer (Vario EL III, Elementar, Germany). Leaf mass per area (LMA, g m^{-2}) was determined from leaf area and leaf dry mass, and leaf nitrogen content per area (N_{area}, g N m^{-2}) was calculated as a product of N_{mass} and LMA.

Analysis of leaf-level and whole-plant stomatal dynamics

Whole-plant and leaf-level stomatal characteristics were characterized by a dynamic sigmoidal model (Vialet-Chabrand et al., 2013). To obtain time constants for stomatal opening and closure, the temporal responses of g_s to increased or decreased PPFD were fitted to the following equations, respectively:

$$g_s = (G_{smax} - r_{open})e^{-e^{\left(\frac{-t}{k_{open}} + 1\right)}} + r_{open} \quad (4)$$

$$g_s = (G_{smin} - r_{close})e^{-e^{\left(\frac{-t}{k_{close}} + 1\right)}} + r_{close} \quad (5)$$

where r_{open} and r_{close} are initial values of g_s before the change in PPFD, G_{smax} and G_{smin} are steady-state maximum or minimum g_s, and k_{open} and k_{close} are time constants indicating rapidity of stomatal opening or closure. We did not use initial time lags for stomatal opening or closure in Equation (4) or (5) since the plants used in the present study showed almost no time lag (Figure 1).

Maximum rate of g_s opening to an increase in PPFD (SI_{open}, mmol m^{-2} s^{-2}) and that to a decrease in PPFD (SI_{close}, −mmol m^{-2} s^{-2}) were calculated as follows:

$$SI_{open} = \frac{(G_{smax} - r_{open})}{k_{open} * e} \quad (6)$$

$$SI_{close} = \frac{(G_{smin} - r_{close})}{k_{close} * e} \quad (7)$$

Stomatal characteristics at the whole-plant level were determined for each light cycle from the temporal response of whole-plant g_s obtained at 30-min intervals of light fluctuation. Meanwhile, they were not determined at 15-min intervals of light fluctuation since g_s did not reach steady-state in most of C_3 crops throughout a day. Leaf-level stomatal characteristics were also determined for the first and second light cycles and averaged for each plant.

Dynamic photosynthesis model in controlled fluctuating light environments

Dynamic photosynthesis model was developed by incorporating the model describing dynamics of g_s (Vialet-Chabrand et al., 2013) with CO_2 assimilation models for C_3 photosynthesis (Farquhar et al., 1980) and C_4 photosynthesis (von Caemmerer, 2000). Using the model, we simulated the effect of changes in k_{open} and k_{close} on A, E, and WUE in the C_3 and C_4 species. Model description is based on Osborne and Sack (2012), and A is determined for a given PPFD and g_s in both C_3 and C_4 species.

For C_3 species, A is expressed as the minimum of either the Rubisco-limited rate of photosynthesis (A_c) or the RuBP regeneration-limited rate of photosynthesis (A_j):

$$A = \min(A_c, A_j) - R_d \quad (8)$$

where R_d is the mitochondrial respiration rate. A_c is expressed as:

$$A_c = \frac{V_{cmax}(C_m - \Gamma^*)}{C_m + K_c(1 + O/K_o)} \quad (9)$$

where V_{cmax} is the maximum rate of RuBP carboxylation, C_m is the CO_2 concentration in mesophyll cells, Γ^* is the CO_2 compensation point in the absence of R_d, K_c, and K_o are the Michaelis constants for CO_2 and O_2, respectively, and O is the O_2 concentration. A_j is expressed as:

$$A_j = \frac{J(C_m - \Gamma^*)}{4(C_m + 2\Gamma^*)} \quad (10)$$

where J is the electron transport rate expressed as follows:

$$J = \frac{\Phi_r \text{ PPFD} + J_{max} - \sqrt{(\Phi_r \text{ PPFD} + J_{max})^2 - 4\Phi_r \text{ PPFD } \theta_r J_{max}}}{2\theta_r} \quad (11)$$

where Φ_r is the initial slope of the curve, J_{max} is the maximum electron transport rate, and θ_r is the convexity of the curve. The equation indicates that A_j is greatly affected by PPFD. A is also expressed as follows:

$$A = g_t(C_a - C_m) \quad (12)$$

where C_a is the atmospheric CO_2 concentration and g_t is the total CO_2 conductance from the atmosphere to the mesophyll cells:

$$\frac{1}{g_t} = \frac{1}{g_{sc}} + \frac{1}{g_{mc}} \quad (13)$$

where stomatal conductance for CO_2 (g_{sc}) is g_s/1.6, and mesophyll conductance for CO_2 (g_{mc}) is $1.65 \times (1.6 \times g_{sc})$ (Vico and Porporato, 2008; Osborne and Sack, 2012). A is determined as the intersection of the demand functions (Eqs. (9) and (10)) and the supply function (Eq. (12)).

For C_4 species, PEP carboxylation is considered as the first step of the C_4 photosynthesis and expressed as follows:

$$V_p = \min\left(\frac{C_m V_{pmax}}{C_m + K_p}, V_{pr}\right) \quad (14)$$

where V_{pmax} is the maximum PEP carboxylation rate, K_p is the Michaelis–Menten constant of PEPC for CO_2, and V_{pr} is an upper bound of V_p limited by PEP regeneration rate. For a given g_s, the C_m that determines PEP carboxylation rate can be obtained by equating Equations (14) and (12) assuming A as V_p. For C_4 species, A is a function of the CO_2 concentration in the bundle sheath cells (C_{bs}) where carbon fixation occurs, and A is expressed as follows:

$$A = V_p - L_{bs} \quad (15)$$

where L_{bs} is the rate of CO_2 leakage from the bundle sheath to the mesophyll, which is expressed as follows:

$$L_{bs} = g_{bs}(C_{bs} - C_m) \quad (16)$$

where g_{bs} is the bundle sheath conductance of CO_2. Finally, A is determined as the intersection of Equations (15) and (9) or (10), where C_m is replaced with C_{bs} for C_4 species.

In addition, E is calculated from g_s and VPD as follows:

$$E = g_s \frac{VPD}{101.3} \quad (17)$$

where VPD is obtained using Equation (3).

We selected *T. aestivum* with larger k_{open} and k_{close} and *E. coracana* with the smallest k_{open} and k_{close} as representatives of C_3 and C_4 species, respectively. We firstly checked the accuracy of the model prediction in the controlled fluctuating light environments in *T. aestivum* and *E. coracana* using parameters obtained from the present and previous studies (von Caemmerer, 2000; Vico and Porporato, 2008; Osborne and Sack, 2012; Table 2). We then simulated the dynamics of A, E, g_s, and WUE in *T. aestivum* and *E. coracana* with original and altered k_{open} and k_{close}. The effects of decreasing k_{open} and k_{close} separately or simultaneously in *T. aestivum* and those of increasing k_{open} and k_{close} separately or simultaneously in *E. coracana* on total photosynthesis (A_{total}, mmol CO_2 m^{-2}), total transpiration (E_{total}, mol H_2O m^{-2}), and total WUE (WUE_{total}, mmol CO_2 mol H_2O^{-1}) as the ratio of A_{total} to E_{total} during the 75-min fluctuating light period were evaluated.

Statistical analysis

Statistical tests were performed using R (http://www.r-project.org/). Significant differences in the physiological and morphological characteristics among species were determined by one-way ANOVA followed by a Tukey–Kramer. The effects of photosynthetic types (C_3 or C_4), soil nitrogen conditions, and their interaction on the characteristics were determined by two-way ANOVA.

Supplemental data

The following materials are available in the online version of this article.

Supplemental Figure S1. Maximum slope of the response of stomatal conductance (g_s) to the increased PPFD (SI_{open}) and that to the decreased PPFD (SI_{close}) in four C_3 and five C_4 species grown under HN or LN conditions.

Supplemental Figure S2. Relationship between mean SD_{mean} and mean GL_{mean} in four C_3 and five C_4 species grown under HN or LN conditions.

Supplemental Figure S3. Dynamics of the whole-plant stomatal conductance (g_s) in the controlled fluctuating light environments in four C_3 species.

Supplemental Figure S4. Dynamics of the whole-plant stomatal conductance (g_s) in the controlled fluctuating light environments in five C_4 species.

Supplemental Figure S5. Relationship between whole-plant and leaf-level stomatal characteristics in four C_3 and five C_4 species grown under HN or LN conditions.

Supplemental Figure S6. Relationship between the CO_2 assimilation rate (A_c, A_j, V_p) and CO_2 concentration in mesophyll cells (C_m) or bundle sheath cells (C_{bs}) described by the C_3 or C_4 photosynthesis models.

Supplemental Figure S7. Changes in stomatal conductance (g_s), photosynthetic rate (A), transpiration rate (E), and (A/E) in the controlled fluctuating light environments simulated by the dynamic photosynthesis model in *T. aestivum* (A–H) and *E. coracana* (I–P) grown under HN conditions.

Supplemental Figure S8. Relationship between WUE during high (WUE_{HL}) and low light period (WUE_{LL}) and time constants for stomatal opening (k_{open}) and closure (k_{close}) in four C_3 and five C_4 species grown under HN or LN conditions.

Supplemental Figure S9. Experimental design for evaluating whole-plant water consumption in controlled fluctuating light environments.

Supplemental Figure S10. Changes in leaf temperature (T_L) in the fluctuating light environments at 30-min intervals in *T. aestivum* and *E. coracana*.

Supplemental Table S1. Stomatal characteristics determined by the photosynthesis measurements in four C_3 species and five C_4 species.

Supplemental Table S2. Physiological and morphological characteristics of the leaves used for the photosynthesis measurements in four C_3 species and five C_4 species.

Supplemental Table S3. Whole-plant water use characteristics determined by the continuous measurements of pot weight in the controlled fluctuating environment in four C_3 species and five C_4 species.

Acknowledgments

We thank Mr Kato, Dr Oi, Dr Mano, Dr Takahashi, and Dr Nakazono for sharing plant materials and Mr Kinoshita for developing the automatic logging application for the Bluetooth communication balance. We also thank the members of Crop Science laboratory in Nagoya University for their valuable comments and encouragement.

Funding

This study was supported by a grant for basic science research project from the Sumitomo Foundation (Grant No. 190909) and Toray science foundation (Grant No. 17-5800).

Conflict of interest statement. None declared.

References

Barratt GE, Sparkes DL, McAusland L, Murchie EH (2021) Anisohydric sugar beet rapidly responds to light to optimize leaf water use efficiency utilizing numerous small stomata. AoB Plants **13:** plaa067

Bellasio C, Quirk J, Buckley TN, Beerling DJ (2017) A dynamic hydro-mechanical and biochemical model of stomatal conductance for C_4 photosynthesis. Plant Physiol **175:** 104–119

Beaulieu JM, Leitch IJ, Patel S, Pendharkar A, Knight CA (2008) Genome size is a strong predictor of cell size and stomatal density in angiosperms. New Phytol **179:** 975–986

Cano FJ, Sharwood RE, Cousins AB, Ghannoum O (2019) The role of leaf width and conductances to CO_2 in determining water use efficiency in C_4 grasses. New Phytol **223:** 1280–1295

Carrão H, Naumann G, Barbosa P (2016) Mapping global patterns of drought risk: an empirical framework based on sub-national estimates of hazard, exposure and vulnerability. Glob Environ Change **39:** 108–124

Clearwater MJ, Luo Z, Mazzeo M, Dichio B (2009) An external heat pulse method for measurement of sap flow through fruit pedicels, leaf petioles and other small-diameter stems. Plant Cell Environ **32:** 1652–1663

Condon AG (2020) Drying times: plant traits to improve crop water use efficiency and yield. J Exp Bot **71:** 2239–2252

Dai Z, Ku MSB, Edwards GE (1993) C_4 photosynthesis (the CO_2-concentrating mechanism and photorespiration). Plant Physiol **103:** 83–90

Daloso DM, Dos Anjos L, Fernie AR (2016) Roles of sucrose in guard cell regulation. New Phytol **211:** 809–818

Douthe C, Medrano H, Tortosa I, Escalona JM, Hernández-Montes E, Pou A (2018) Whole-plant water use in field grown grapevine: seasonal and environmental effects on water and carbon balance. Front Plant Sci **9:** 1540

Drake PL, Froend RH, Franks PJ (2013) Smaller, faster stomata: scaling of stomatal size, rate of response, and stomatal conductance. J Exp Bot **64:** 495–505

Elliott-Kingston C, Haworth M, Yearsley JM, Batke SP, Lawson T, McElwain JC (2016) Does size matter? Atmospheric CO_2 may be a stronger driver of stomatal closing rate than stomatal size in taxa that diversified under low CO_2. Front Plant Sci **7:** 1253

Evans JR (1989) Photosynthesis and nitrogen relationships in leaves of C_3 plants. Oecologia **78:** 9–19

Eyland D, van Wesemael J, Lawson T, Carpentier S (2021) The impact of slow stomatal kinetics on photosynthesis and water use efficiency under fluctuating light. Plant Physiol **186:** 998–1012

Farquhar GD, von Caemmerer S, Berry JA (1980) A biochemical model of photosynthetic CO_2 assimilation in leaves of C_3 species. Planta **149:** 78–90

Gallaher RN, Ashley DA, Brown RH (1975) ^{14}C-photosynthate translocation in C_3 and C_4 plants as related to leaf anatomy. Crop Sci **15:** 55–59

Ghannoum O, von Caemmerer S, Conroy JP (2002) The effect of drought on plant water use efficiency of nine NAD-ME and nine NADP-ME Australian C_4 grasses. Funct Plant Biol **29:** 1337–1348

Ghannoum O, Evans JR, von Caemmerer S (2011) Nitrogen and water use efficiency of C_4 plants. In AS Raghavendra, RF Sage, eds, C_4 Photosynthesis and Related CO_2 Concentrating Mechanisms. Springer, Dordrecht, The Netherlands, pp 129–146

Granier A (1987) Evaluation of transpiration in a Douglas-fir stand by means of sap flow measurements. Tree Physiol **3:** 309–320

Gray A, Liu L, Facette M (2020) Flanking support: how subsidiary cells contribute to stomatal form and function. Front Plant Sci **11:** 881

Grodzinski B, Jiao J, Leonardos ED (1998) Estimating photosynthesis and concurrent export rates in C_3 and C_4 species at ambient and elevated CO_2. Plant Physiol **117:** 207–215

Gutierrez M, Gracen VE, Edwards GE (1974) Biochemical and cytological relationships in C_4 plants. Planta **119:** 279–300

Henderson SA, Hattersley P, von Caemmerer S, Osmond CB (1994) Are C_4 pathway plants threatened by global climatic change? *In* ED Schulze, MM Caldwell, eds, Ecophysiology of Photosynthesis. Springer, Berlin, pp 529–549

Higaki T, Hashimoto-Sugimoto M, Akita K, Iba K, Hasezawa S (2014) Dynamics and environmental responses of PATROL1 in *Arabidopsis* subsidiary cells. Plant Cell Physiol **55:** 773–780

Hikosaka K, Ishikawa K, Borjigidai A, Muller O, Onoda Y (2006) Temperature acclimation of photosynthesis: mechanisms involved in the changes in temperature dependence of photosynthetic rate. J Exp Bot **57:** 291–302

Hirabayashi Y, Mahendran R, Koirala S, Konoshima L, Yamazaki D, Watanabe S, Kim H, Kanae S (2013) Global flood risk under climate change. Nat Clim Change **3:** 816–821

Igarashi M, Yi Y, Yano K (2021) Revisiting why plants become N deficient under elevated CO_2: importance to meet N demand regardless of the fed-form. Front Plant Sci **12:** 726186

Israel WK, Watson-Lazowski A, Chen Z-H, Ghannoum O (2021) High intrinsic water use efficiency is underpinned by high stomatal aperture and guard cell potassium flux in C_3 and C_4 grasses grown at glacial CO_2 and low light. J Exp Bot (In press).

Kimura H, Hashimoto-Sugimoto M, Iba K, Terashima I, Yamori W (2020) Improved stomatal opening enhances photosynthetic rate and biomass production in fluctuating light. J Exp Bot **71:** 2339–2350

Lawson T, Blatt MR (2014) Stomatal size, speed, and responsiveness impact on photosynthesis and water use efficiency. Plant Physiol **164:** 1556–1570

Lawson T, Vialet-Chabrand S (2019) Speedy stomata, photosynthesis and plant water use efficiency. New Phytol **221:** 93–98

Lawson T, Matthews J (2020) Guard cell metabolism and stomatal function. Annu Rev Plant Biol **71:** 273–302

Leakey ADB, Ferguson JN, Pignon CP, Wu A, Jin Z, Hammer GL, Lobell DB (2019) Water use efficiency as a constraint and target for improving the resilience and productivity of C_3 and C_4 crops. Annu Rev Plant Biol **70:** 781–808

Lundgren MR, Mathers A, Baillie AL, Dunn J, Wilson MJ, Hunt L, Pajor R, Fradera-Soler M, Rolfe S, Osborne CP, et al. (2019) Mesophyll porosity is modulated by the presence of functional stomata. Nat Commun **10:** 2825

McAusland L, Vialet-Chabrand S, Davey P, Baker NR, Brendel O, Lawson T (2016) Effects of kinetics of light-induced stomatal responses on photosynthesis and water-use efficiency. New Phytol **211:** 1209–1220

McNaughton KG, Jarvis PG. (1991) Effects of spatial scale on stomatal control of transpiration. Agric For Meteorol **54:** 279–302

Miyashita A, Sugiura D, Sawakami K, Ichihashi R, Tani T, Tateno M (2012) Long-term, short-interval measurements of the frequency distributions of the photosynthetically active photon flux density and net assimilation rate of leaves in a cool-temperate forest. Agric For Meteorol **152:** 1–10

Monsi M, Saeki T (2005) On the factor light in plant communities and its importance for matter production. Ann Bot **95:** 549–567

Osborne CP, Sack L (2012) Evolution of C_4 plants: a new hypothesis for an interaction of CO_2 and water relations mediated by plant hydraulics. Phil Trans R Soc B **367:** 583–600

Papanatsiou M, Petersen J, Henderson L, Wang Y, Christie JM, Blatt MR (2019) Optogenetic manipulation of stomatal kinetics

improves carbon assimilation, water use, and growth. Science **363:** 1456–1459

Pearcy RW (1990) Sunflecks and photosynthesis in plant canopies. Annu Rev Plant Biol **41:** 421–453

Qu M, Hamdani S, Li W, Wang S, Tang J, Chen Z, Song Q, Li M, Zhao H, Chang T (2016) Rapid stomatal response to fluctuating light: an under-explored mechanism to improve drought tolerance in rice. Funct Plant Biol **43:** 727–738

Qu M, Essemine J, Xu J, Ablat G, Perveen S, Wang H, Chen K, Zhao Y, Chen G, Chu C (2020) Alterations in stomatal response to fluctuating light increase biomass and yield of rice under drought conditions. Plant J **104:** 1334–1347

Raissig MT, Matos JL, Gil MXA, Kornfeld A, Bettadapur A, Abrash E, Allison HR, Badgley G, Vogel JP, Berry JA (2017) Mobile MUTE specifies subsidiary cells to build physiologically improved grass stomata. Science **355:** 1215–1218

Rosegrant MW, Ringler C, Zhu T (2009) Water for agriculture: maintaining food security under growing scarcity. Annu Rev Environ Resour **34:** 205–222

Scafaro AP, Von Caemmerer S, Evans JR, Atwell BJ (2011) Temperature response of mesophyll conductance in cultivated and wild *Oryza* species with contrasting mesophyll cell wall thickness. Plant Cell Environ **34:** 1999–2008

Schneider CA, Rasband WS, Eliceiri KW (2012) NIH Image to ImageJ: 25 years of image analysis. Nat Methods **9:** 671

Schulze E-D, Ellis R, Schulze W, Trimborn P, Ziegler H (1996) Diversity, metabolic types and $\delta^{13}C$ carbon isotope ratios in the grass flora of Namibia in relation to growth form, precipitation and habitat conditions. Oecologia **106:** 352–369

Shantz HL, Piemeisel LN (1927) The water requirements of plants at Akron. Colorado J Agric Res **34:** 1093–1190

Shimazaki K, Doi M, Assmann SM, Kinoshita T (2007) Light regulation of stomatal movement. Annu Rev Plant Biol **58:** 219–247

Silva-Pérez V, Furbank RT, Condon AG, Evans JR (2017) Biochemical model of C_3 photosynthesis applied to wheat at different temperatures. Plant Cell Environ **40:** 1552–1564

Sugiura D, Betsuyaku E, Terashima I (2019) Interspecific differences in how sink-source imbalance causes photosynthetic downregulation among three legume species. Ann Bot **123:** 715–726

Sugiura D, Terashima I, Evans JR (2020) A decrease in mesophyll conductance by cell wall thickening contributes to photosynthetic down-regulation. Plant Physiol **183:** 1600–1611

Talbott LD, Zeiger E (1998) The role of sucrose in guard cell osmoregulation. J Exp Bot **49:** 329–337

Talwar HS, Kumar S, Madhusudhana R, Nanaiah GK, Ronanki S, Tonapi VA (2020) Variations in drought tolerance components and their association with yield components in finger millet (*Eleusine coracana*). Funct Plant Biol **47:** 659–674

Taylor SH, Franks PJ, Hulme SP, Spriggs E, Christin PA, Edwards EJ, Woodward FI, Osborne CP (2012) Photosynthetic pathway and ecological adaptation explain stomatal trait diversity amongst grasses. New Phytol **193:** 387–396

Trtikova M, Lohn A, Binimelis R, Chapela I, Oehen B, Zemp N, Widmer A, Hilbeck A (2017) Teosinte in Europe-searching for the origin of a novel weed. Sci Rep **7:** 1560

Tsutsumi N, Tohya M, Nakashima T, Ueno O (2017) Variations in structural, biochemical, and physiological traits of photosynthesis and resource use efficiency in *Amaranthus* species (NAD-ME-type C_4). Plant Prod Sci **20:** 300–312

Vialet-Chabrand S, Dreyer E, Brendel O (2013) Performance of a new dynamic model for predicting diurnal time courses of stomatal conductance at the leaf level. Plant Cell Environ **36:** 1529–1546

Vico G, Porporato A (2008) Modelling C_3 and C_4 photosynthesis under water-stressed conditions Plant Soil **313:** 187–203

Vico G, Manzoni S, Palmroth S, Katul G (2011) Effects of stomatal delays on the economics of leaf gas exchange under intermittent light regimes. New Phytol **192:** 640–652

Vogan PJ, Sage RF (2011) Water-use efficiency and nitrogen-use efficiency of C_3-C_4 intermediate species of *Flaveria Juss.* (*Asteraceae*). Plant Cell Environ **34:** 1415–1430

von Caemmerer S (2000) Biochemical Models of Leaf Photosynthesis, Collingwood, Australia, CSIRO Publishing

Wang Y, Chan KX, Long SP (2021) Toward a dynamic photosynthesis model to guide yield improvement in C_4 crops. Plant J (In press)

Way DA, Katul GG, Manzoni S, Vico G (2014) Increasing water use efficiency along the C_3 to C_4 evolutionary pathway: a stomatal optimization perspective. J Exp Bot **65:** 3683–3693

Yamori W, Masumoto C, Fukayama H, Makino A (2012) Rubisco activase is a key regulator of non-steady-state photosynthesis at any leaf temperature and, to a lesser extent, of steady-state photosynthesis at high temperature. Plant J **71:** 871–880

Yamori W, Kusumi K, Iba K, Terashima I (2020) Increased stomatal conductance induces rapid changes to photosynthetic rate in response to naturally fluctuating light conditions in rice. Plant Cell Environ **43:** 1230–1240

Zhang Q, Peng S, Li Y (2019) Increase rate of light-induced stomatal conductance is related to stomatal size in the genus *Oryza*. J Exp Bot **70:** 5259–5269